1973

Calculation of gamma-ray albedo using the Monte Carlo method

Ezatholah Aslani-Amoli

CALCULATION OF GAMMA-RAY ALBEDO USING THE MONTE CARLO METHOD

by

EZATHOLAH ASLANI-AMOLI, 1945-

A THESIS

Presented to the Faculty of the Graduate School of the

UNIVERSITY OF MISSOURI-ROLLA

In Partial Fulfillment of the Requirements for the Degree

MASTER OF SCIENCE IN NUCLEAR ENGINEERING

1973

Approved by


(Advisor)

ABSTRACT

Gamma-ray number, energy and dose albedo are calculated with the Monte Carlo technique. A plane monoenergetic beam was considered at normal incidence upon single material shields at initial gamma energy up to 10 MeV. Aluminum, iron and lead are used as shield material. The contribution of secondary photons which are produced as a result of various photon interactions in the shield are taken into account. These secondary photons are annihilation gammas, X rays and bremsstrahlung gammas. In certain cases, they constitute a considerable fraction of the reflected radiation.

Annihilation gammas predominate in the reflected radiation for all energies above 1.02 MeV. For example, in the case of 8 MeV photons incident on lead, 96% of the reflected particles are .511 annihilation gammas.

The X-ray contribution to albedo is more pronounced at low energy and high Z material. For example, this contribution is 57% to number albedo, 94% to energy albedo and 38% to dose albedo for .41 MeV photons incident on lead.

Bremsstrahlung contribution increases both with atomic number Z and photon energy. It amounts to 13% of number albedo, 24% of energy albedo and 23% of dose albedo for 10 MeV photons incident on lead.

ACKNOWLEDGMENT

This work has been made possible with the skillful guidance of my advisor, Dr. Nick Tsoulfanidis. His valuable experience and insight in research work enabled the successful completion of this work. His continuous encouragement and advise are greatly appreciated.

The assistance of Dr. D. R. Edwards, head of nuclear engineering program, is deeply appreciated.

Mr. John Kuspa participated in many helpful discussions and his work on Gamma Ray Buildup Factor Calculation was a great assistance. Mr. Glenn Schade was helpful in some details of the computer programming.

TABLE OF CONTENTS

LIST OF ILLUSTRATIONS

LIST OF ILLUSTRATIONS (cont.)

LIST OF TABLES

I. INTRODUCTION

In optics and astronomy the reflection of light waves on a material can be considered a surface phenomenon and its diffuse reflection is defined as albedo. In contrast, nuclear radiation (such as neutrons and gammas) penetrates the medium deeper than its surface and its reflection from that medium encompasses radiation that is scattered one or more times inside the medium. Mathematically the fraction of radiation being reflected, called albedo, has been defined in several ways[1,2,3]. In the present work the concept of albedo will be defined for gamma rays. Figure 1 shows the geometry considered.

Let $J(E_0,\theta_0)$ be the incident radiation current consisting of monoenergetic photons with energy E_0(MeV) and incident at a polar angle θ_0. Let $J(E,\theta,\phi)$ be the reflected current per unit solid angle in the direction defined by (θ,ϕ) per unit energy at energy E. Then, double differential albedo, $\alpha(E_0,\theta_0,E,\theta,\phi)$ is defined as follows

$$\alpha(E_0,\theta_0,E,\theta,\phi) = \frac{J(E_0,\theta_0,E,\theta,\phi)}{J(E_0,\theta_0)} \tag{1}$$

In other words, $\alpha(E_0,\theta_0,E,\theta,\phi)$ is the fraction of incident current backscattered per unit solid angle per unit energy. In the present work only normally incident radiation was considered. Therefore, the albedo is independent of ϕ. In what follows, the albedo will be indicated as a function of E_0, E, and θ only. Depending on the

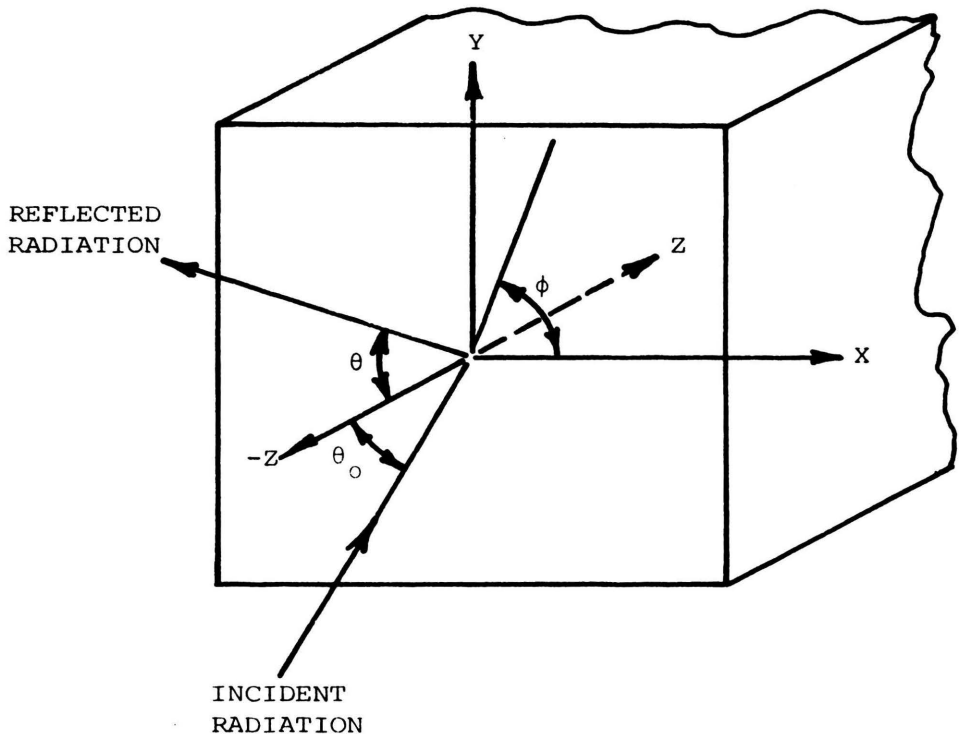

Fig. 1. Geometry Considered in the Definition of Albedo.

type of the incident current (Number, Energy or Dose) number, energy and dose albedo is defined as shown below, with the subscript indicating the type of albedo.

$$\alpha_N(E_0,E,\theta) = \frac{J_N(E_0,E,\theta)}{J_N(E_0)} \quad MeV^{-1}\cdot str^{-1} \tag{2}$$

$$\alpha_E(E_0,E,\theta) = \frac{J_E(E_0,E,\theta)}{J_E(E_0)} \quad MeV^{-1}\cdot str^{-1} \tag{3}$$

$$\alpha_D(E_0,E,\theta) = \frac{J_D(E_0,E,\theta)}{J_D(E_0)} \quad MeV^{-1}\cdot str^{-1} \tag{4}$$

Integration of $\alpha_N(E_0,E,\theta)$, $\alpha_E(E_0,E,\theta)$ and $\alpha_D(E_0,E,\theta)$ over the solid angle $d\Omega = 2\pi\sin\theta d\theta (0 < \theta \leq \pi/2)$ results in the differential energy-dependent number, energy or dose albedo. For example, the differential energy-dependent number albedo is

$$\alpha_N(E_0,E) = \int_{2\pi} \alpha_N(E_0,E,\theta)d\Omega = 2\pi \int_0^{\pi/2} \alpha_N(E_0,E,\theta)\sin\theta d\theta \tag{5}$$

Obviously, $\alpha_N(E_0,E)$ gives the energy spectrum of the reflected particles.

Integration of the double differential albedo over energy gives the differential angle-dependent albedo-number energy or dose. For example, the differential angle-dependent number albedo is:

$$\alpha_N(E_0,\theta) = \int_0^{E_0} \alpha_N(E_0,E,\theta)dE \tag{6}$$

Equation 1 gives essentially the angular distribution of reflected particles.

The total albedo, which is the ratio of total reflected output-number, energy or dose-to corresponding total input, is obtained by double iterated as follows:

$$\alpha_N(E_0) = 2\pi \int_0^{\pi/2} \sin\theta d\theta \int_0^{E_0} \alpha_N(E_0,E,\theta)dE \tag{7}$$

$$\alpha_E(E_0) = 2\pi \int_0^{\pi/2} \sin\theta d\theta \int_0^{E_0} \alpha_E(E_0,E,\theta)dE \tag{8}$$

$$\alpha_D(E_0) = 2\pi \int_0^{\pi/2} \sin\theta d\theta \int_0^{E_0} \alpha_D(E_0,E,\theta)dE \tag{9}$$

In the present work, a computer program was developed which calculates double and single differential as well as total albedo and energy deposition pattern inside a shielding material for normally incident gamma rays with energy up to 10 MeV. Multiple layer shield case could also be studied by this program.

Gamma-ray albedo has been studied in the past both theoretically and experimentally by many people[4-24]. Due to lack of an adequate number of monoenergetic gamma-ray sources, most experimental albedo determinations[2,5-9] are for .41 MeV, .66 MeV and 1.25 MeV which correspond to gamma energies emitted by the isotopes Au-198, Cs-137 and Co-60 respectively. Only very recently Johnson[10-12] and his

co-workers have measured albedo for energies up to 8 MeV utilizing capture gammas produced by titanium target bombarded with neutrons.

For the theoretical calculation of albedo, two methods have been generally used. One is Monte-Carlo method[13-23], the other is the moments method[25]. The moments method has the disadvantage that it cannot adequately handle secondary particles, besides the discrepancy it has shown due to boundary effects. The Monte-Carlo method was chosen for the present study because of its flexibility for consideration of all secondary particles produced by the incident photons. The secondary photons considered are (a) annihilation gammas (b) X rays emitted by atoms participating in photoelectric interaction and (c) bremsstrahlung emitted by electrons and positrons. Bremsstrahlung was considered in great detail, something that has not been adequately done in the past. In addition, the effect of coherent scattering (Rayleigh scattering) and non-coherent scattering (Compton scattering) was examined individually. The results indicate that in many cases the secondary radiations contribute a significant fraction to the values of albedo.

II. DESCRIPTION OF THE MONTE-CARLO PROGRAM

A. General Description

Based on the Monte-Carlo technique, a computer program was developed for a multilayer slab shield, up to three layers, with cross sectional dimensions of 65 cm x 65 cm and variable thickness. A normally incident monoenergetic gamma-ray circular beam, with radius of 10 cm, and energy range 0-10 MeV was considered. The number of initial photons considered was such that the standard error for total albedo was 10% or less. The number of histories per case varied depending on incident energy and type and thickness of shield. Each photon is followed individually upon entering the shield until either its energy falls below 10 KeV, it is absorbed in the shield or emerges from the shield. Theoretically a photon could have an infinite number of scattering collisions and still survive inside the shield. To avoid unnecessary use of computer time, a maximum of 100 collisions per particle was allowed. This limit was never exceeded in all the cases studied.

All the necessary attenuation coefficients (pair production, photoelectric, Compton scattering, Rayleigh scattering, and total tissue absorption coefficients) were entered as data at regular energy intervals from 0-10 MeV. The values of the coefficients were obtained from tables[26]. Needed values of attenuation coefficients which were not tabulated were obtained by linear interpolation. The explicit contributions of bremsstrahlung and

X rays are indicated by studying the gammas in the shield in what we call three "passes" through the program.

In the first pass, the original gammas and the annihilation photons are considered, partial results due to their contributions are printed out and information about bremsstrahlung and X rays generated is stored. This information consists of position, direction of motion and energy of each photon.

In the second pass, the bremsstrahlung photons are followed and partial results which are the sum of first and second pass are printed out. Thus, by comparing results of the first two passes, the contribution of bremsstrahlung is indicated explicitly. During the second pass, no bremsstrahlung is stored but information about X rays generated in that pass is again stored.

In the third pass, the X rays are considered in the same way as bremsstrahlung in second pass. The results of the third pass are the sum of the three passes through the program.

B. Gamma-ray Tracking

The distance between two successive interactions of a photon with energy E is obtained by using the standard formula $R = -\ell n(RN)/\mu_t(E)$, where $0 \leq RN \leq 1$ is a random number and $\mu_t(E)$ is the total linear attenuation coefficient for a photon of energy E moving in the material of which the shield is made and is equal to:

$$\mu_t(E) = \sum_{i=1}^{4} \mu_i(E) = \mu_{Rs}(E) + \mu_{Cs}(E) + \mu_{Pe}(E) + \mu_{Pp}(E) \qquad (10)$$

The four components of $\mu_t(E)$ represent the coefficients for the four types of interactions considered, Rayleigh scattering, Compton scattering, photoelectric effect and pair production respectively. The type of interaction is determined by utilizing the relative probability of occurrence of event i, $\frac{\mu_i(E)}{\mu_t(E)}$, and comparing it to a random number.

If pair production occurs, the photon history ends. An electron-positron pair is formed with energy $T = E_e = E_p = (E_\gamma - 1.022)/2$. According to theory, the polar angle of emission is $\theta_e = \theta_p = .511/T$ provided $T >> .511$. For lower energies the angular distribution of the pair is more complicated but closer to isotropic. In the present work, the polar angle θ was selected as $\theta_e = \theta_p = .511/T$ for $T \geq .511$ and was selected isotropically for $T < .511$. The azimuthal angles are chosen isotropically with the condition $\phi_e = \phi_p + \pi$. The point of birth of the pair is that of the position of the pair production event. The electron and positron are processed before considering a new history (see section C of this chapter).

If photoelectric effect occurs, the photon history ends and its energy is given to a photoelectron and a X ray. Every atom participating in a photoelectric effect can emit X rays of several energies depending on the energy state from which photoelectron was emitted. Since 80% of the photoelectron processes take place in the K shell, if the photon energy exceeds the K shell binding energy, for simplicity the present work assumed

that photoelectric absorption takes place only in one shell and a X ray of the same energy is always emitted. The energy of the X ray (E_X) was taken equal to the average of all the K X rays of the material. The photoelectron has the remaining energy (E_e)

$$E_e = E_\gamma - E_X \tag{11}$$

The photoelectron's emission angle, relative to the direction of motion of the photon, is obtained by sampling the photoelectron angular distribution curve[27] using Kahn's rejection technique[28]. It is assumed that the X ray is emitted isotropically. The photoelectron is followed inside the shield before studying a new history. The information about the X ray is stored for process in the third pass through the program (see section E of this chapter).

If Compton scattering occurs, which is photon interaction with a free electron, the photon history is continued by following the scattered photon inside the shield. The energy of the scattered photon and the electron are calculated based on a two body collision for which standard kinematics of conservation of energy and momentum apply.

The scattering angle of Compton photon (θ_γ) is selected by applying the Kahn rejection technique to the Klein-Nishina formula[27]. The Compton electron scattering angle, θ_e, is obtained by[27]:

$$\cot(\theta_e) = (1 + \alpha)\tan(\theta_\gamma/2) \tag{12}$$

where $\alpha = E_\gamma(\text{MeV})/.511$. The Compton electron is traced inside the shield before considering a new gamma history.

Rayleigh scattering is elastic coherent scattering by tightly bound atomic electrons. As a result of such an event, a small amount of momentum is imparted to the atom, but no excitation takes place. The Rayleigh scattering angle is small and the energy lost by the photon is also small. The cross section for Rayleigh scattering is relatively large, compared to that for Compton scattering, for small gamma energies and high Z materials. Rayleigh scattering has been neglected in the past because of unimportant change to the photon energy and direction of motion. The Rayleigh cross section was incorporated into the Compton scattering cross section.

The present work considers Rayleigh scattering independently of Compton. When Rayleigh scattering takes place, the photon history is continued with the same energy and direction of motion as before the collision. The results indicate that the way this event is treated is important in some cases.

C. Electron and Positron Tracking

Anytime an electron or positron is formed due to any photon interaction, it is traced for the purpose of energy deposition, annihilation gammas and bremsstrahlung consideration. It is assumed that the particle travels in a straight line and travels a distance equal to its range. A semiempirical formula[29] is used

for electron range calculation. This formula was developed for electrons, but it is good for positron range calculation also, if the positron energy is less than 10 MeV[30], which is the case of our study.

The slab shield is divided into many thin sublayers of equal thickness. Part of the energy of each charged particle (electron or positron) is radiated as bremsstrahlung. This part is deducted first (for detail see next section) and the remaining energy is deposited in those sublayers which the particle traverses. The energy is deposited according to the standard energy loss formula[31]. At the end of the positron range two annihilation gammas, each with energy of .511 MeV, are created and move in opposite directions (back to back). These photons are processed before a new history is started.

D. Bremsstrahlung Consideration

The average energy radiated as bremsstrahlung by an electron of energy E_e in a thick target with atomic number Z is given by a formula of the following type[27,32,33]:

$$E_B = (\text{constant}) Z E_e^2 \qquad (13)$$

There is no general agreement on the value of the constant except that it is of the order of 10^{-4}. The latest experimental work[32,33] suggests a constant which is a slowly varying function of Z and E_e.

The value given by these authors is:

$$\text{constant} = \frac{6.4 \times 10^{-4}}{1 + 6.4 \times 10^{-4} Z E_e (\text{MeV})} \tag{14}$$

In this work we used the formula

$$E_B = \frac{3.64 \times 10^{-4}}{1 + 5.87 \times 10^{-4} Z E_e (\text{MeV})} Z E_e^2 (\text{MeV}) \tag{15}$$

which represents a compromise agreeing best with available theoretical and experimental results.

Bremsstrahlung is emitted with a continuous energy spectrum and maximum energy equal to E_e. To handle the problem efficiently in the computer program, the spectrum was considered as discrete with average energy radiated per electron or positron kept equal to the value given by Equation 15. The model assumes that each electron or positron, radiates up to three bremsstrahlung photons. The energy of each photon is selected based on the bremsstrahlung energy distribution determined experimentally[32]. Reference 32 provides the distribution for Al and Fe for electron energies between 0.5-2.8 MeV. Due to lack of adequate bremsstrahlung energy distribution, this distribution for 2.8 MeV electron is used for the entire range of 0-10 MeV electron energy. Also, the distribution for Fe is used for Pb shield as well.

For the ith positron or electron with kinetic energy E_{ei} the total energy radiated as bremsstrahlung, E_{Bi}, is allowed to be:

$E_{B}{}^{i} \leq E_{ei}$. To meet the condition of Equation 15, the following procedure is taken.

Assume that the three possible bremsstrahlung photons emitted by particle i have energies E_i', E_i'', E_i'''. First E_i' is selected from the bremsstrahlung energy distribution. If $E_i' > E_{ei} - E_{min}$, where E_{min} = 10 KeV, the minimum energy considered, only one bremsstrahlung photon with energy E_i' is stored for particle i and the energy $\Delta_i = E_i' - E_{Bi}$ is recorded. The quantity Δ_i is the excess energy, above E_{Bi} given to bremsstrahlung. If $E_i' < E_{ei} - E_{min}$, then E_i'' is selected like E_i'. If $E_i' + E_i'' \geq E_{ei} - E_{min}$, then only two bremsstrahlung photons with energies E_i' and E_i'' are stored for particle i and $\Delta_i = E_i' + E_i'' - E_{Bi}$ is recorded. If $E_i' + E_i'' < E_{ei} - E_{min}$ three bremsstrahlung photons with energies E_i', E_i'', and E_i''' are emitted with $E_i''' = E_{Bi} - (E_i' + E_i'')$. The excess energy Δ_i is zero in this case.

When particle (i+1) is considered, the current value of Δ_i is taken into account. If $\Delta_i < E_{Bi+1}$, then E_{Bi+1} is replaced by $E_{Bi+1} - \Delta_i$ and particle (i+1) is processed like particle i with this smaller fraction of its energy radiated as bremsstrahlung. If $\Delta_i \geq E_{Bi+1}$, then the excess energy stored is $\Delta_{i+1} = \Delta_i - E_{Bi+1}$ and no bremsstrahlung is emitted by particle (i+1). Thus, for a large number of particles the average energy given off as bremsstrahlung satisfies Equation 15. At the same time photons of any energy between 0 and E_{ei} are emitted.

The birthpoint of each bremsstrahlung photon is chosen randomly along the path of the precursor particle. The direction

of motion of each bremsstrahlung photon is taken the same as its precursor particle, since the emission angle of a bremsstrahlung photon is small[27]. The information for each bremsstrahlung photon produced during the first pass through the program is stored and those photons which have energy above the cut-off energy of 10 KeV are processed in the second pass through the program. Bremsstrahlung photons with energy less than 10 KeV are stored as low bremsstrahlung for the purpose of energy balance calculation.

E. X-ray Consideration

X rays were considered according to the following model. During the photon interactions inside the shield, any time a photoelectric event takes place an X ray is produced provided that the energy of the photon is greater than the X ray energy for the shielding material. This energy (E_X) is calculated as explained in section B of this chapter. The isotropically emitted X ray with energy E_X produced in the first two passes through the program is stored and studied in the third pass.

III. RESULTS

A. General Comments

Differential albedo and total albedo have been calculated for several gamma energies up to 10 MeV. Energy deposition inside the shielding material was also calculated. Aluminum, iron and lead shield with thickness of 4, 3 and 2 mean free paths (mfp) respectively, were considered. These thicknesses make the shield semiinfinite. It should be noted, however, that the thickness of each shield in cm is quite different from that in mfp's at any energy.

The number of photon histories in each case was chosen high enough to maintain the standard error for total albedo around 10% or less. The corresponding error for differential albedo is obviously larger. It could be reduced by studying a much greater number of histories, but that would require more computation time.

Experimental results, when available, are shown for comparison.

B. Differential Angle-Dependent Albedo

Figures 2 to 7 present the angular dependence of albedo for the three shielding materials considered for .41 MeV and 10 MeV photon energy. The curves intend to indicate only trend and are not the result of least square fitting. In general, the angular albedo decreases with angle and is maximum in a direction perpendicular to the surface of the medium. At the low energy of

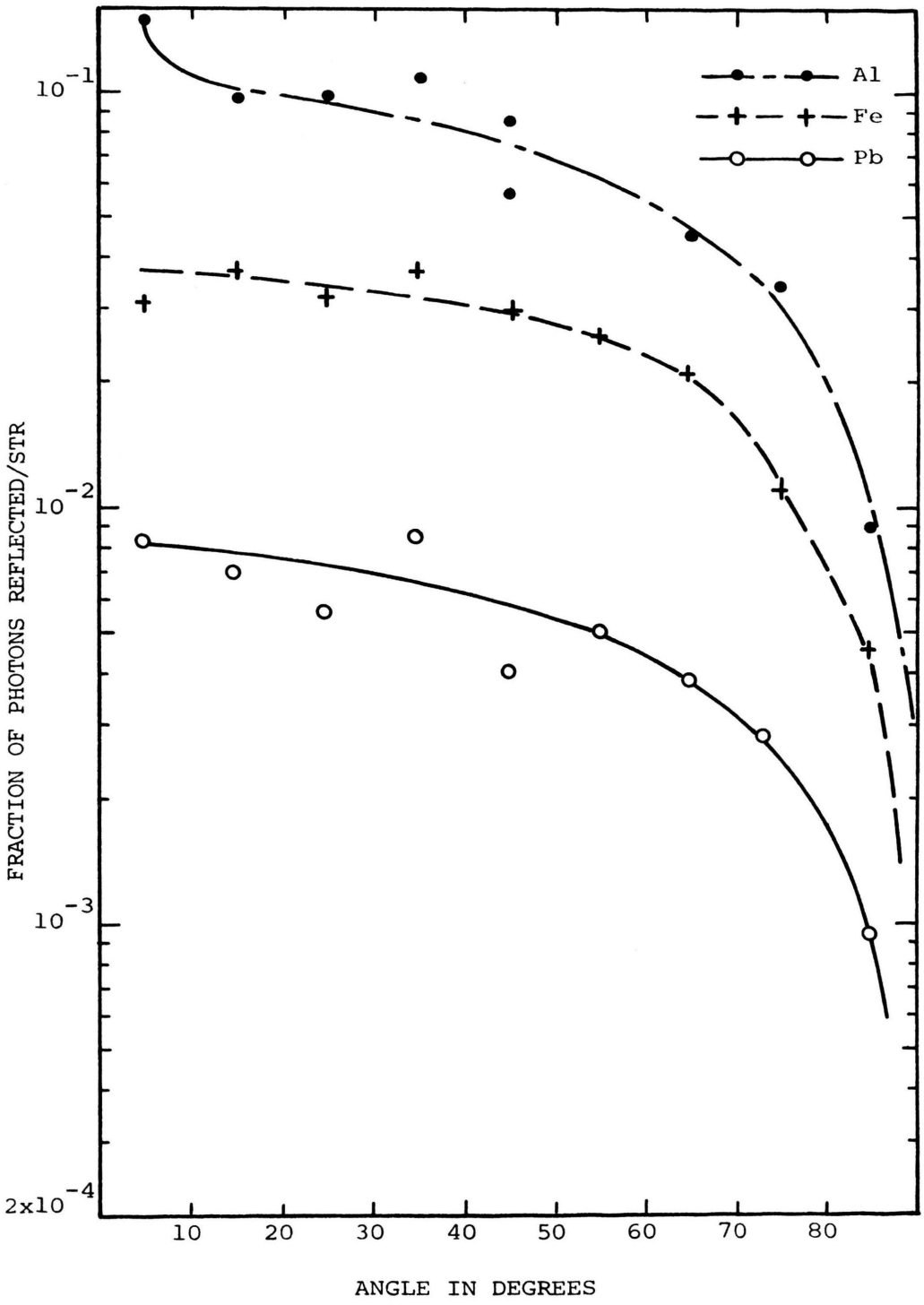

Fig. 2. Differential Number Albedo, $\alpha_N(E_0,\theta)$, for .41 MeV Incident Gammas.

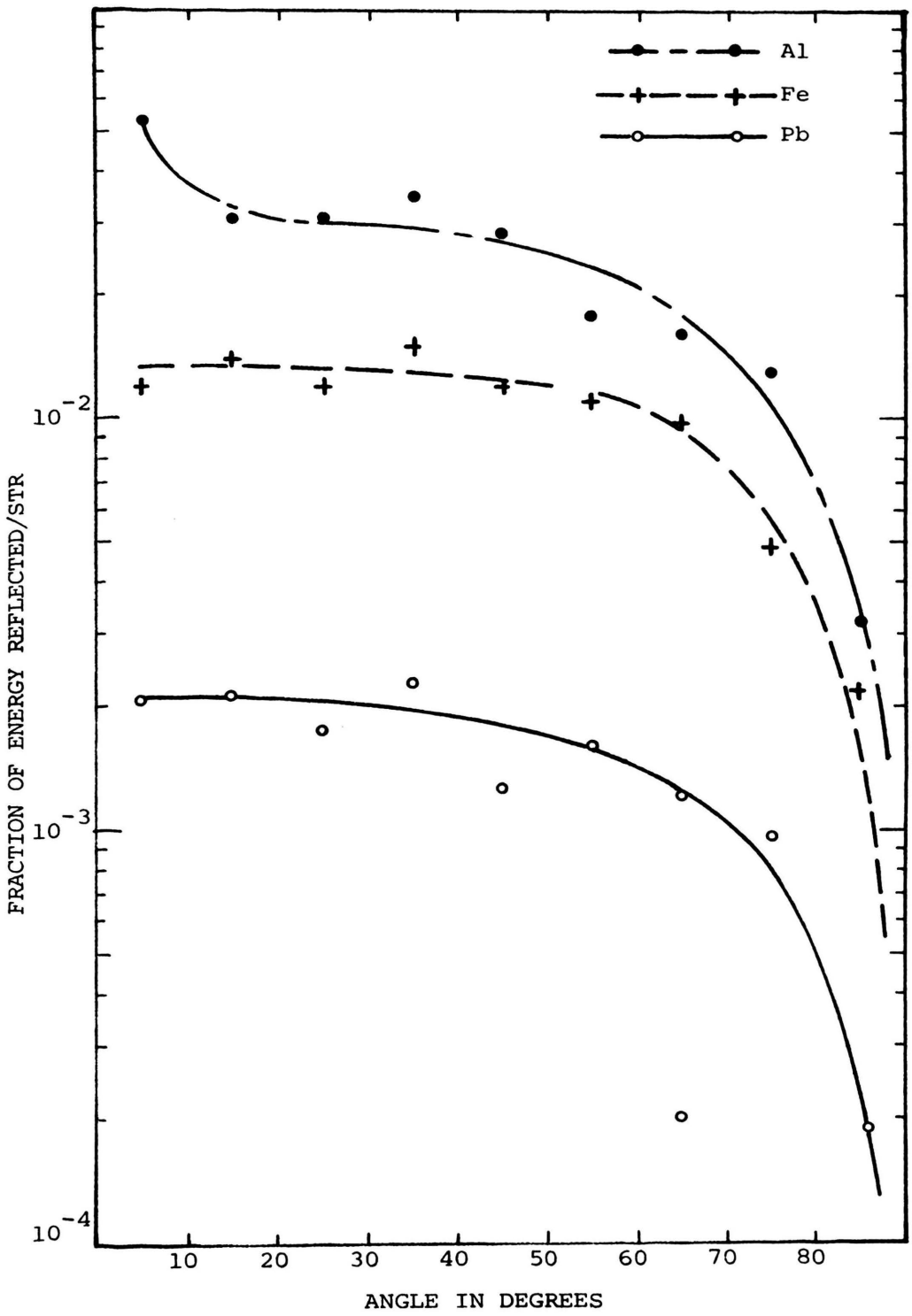

Fig. 3. Differential Energy Albedo, $\alpha_E(E_0,\theta)$, for .41 MeV Incident Gammas.

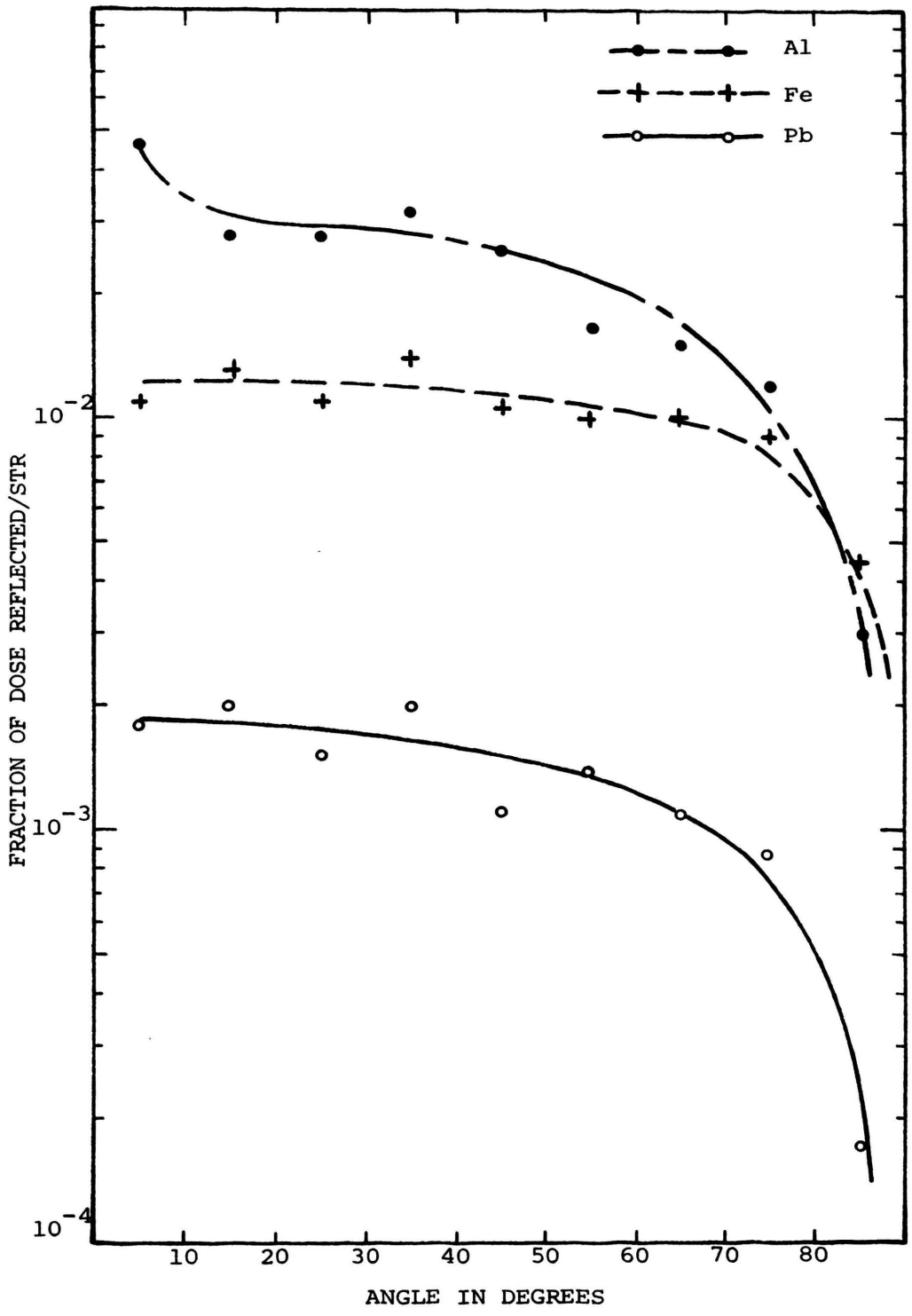

Fig. 4. Differential Dose Albedo, $\alpha_D(E_0,\theta)$, for .41 MeV Incident Gammas.

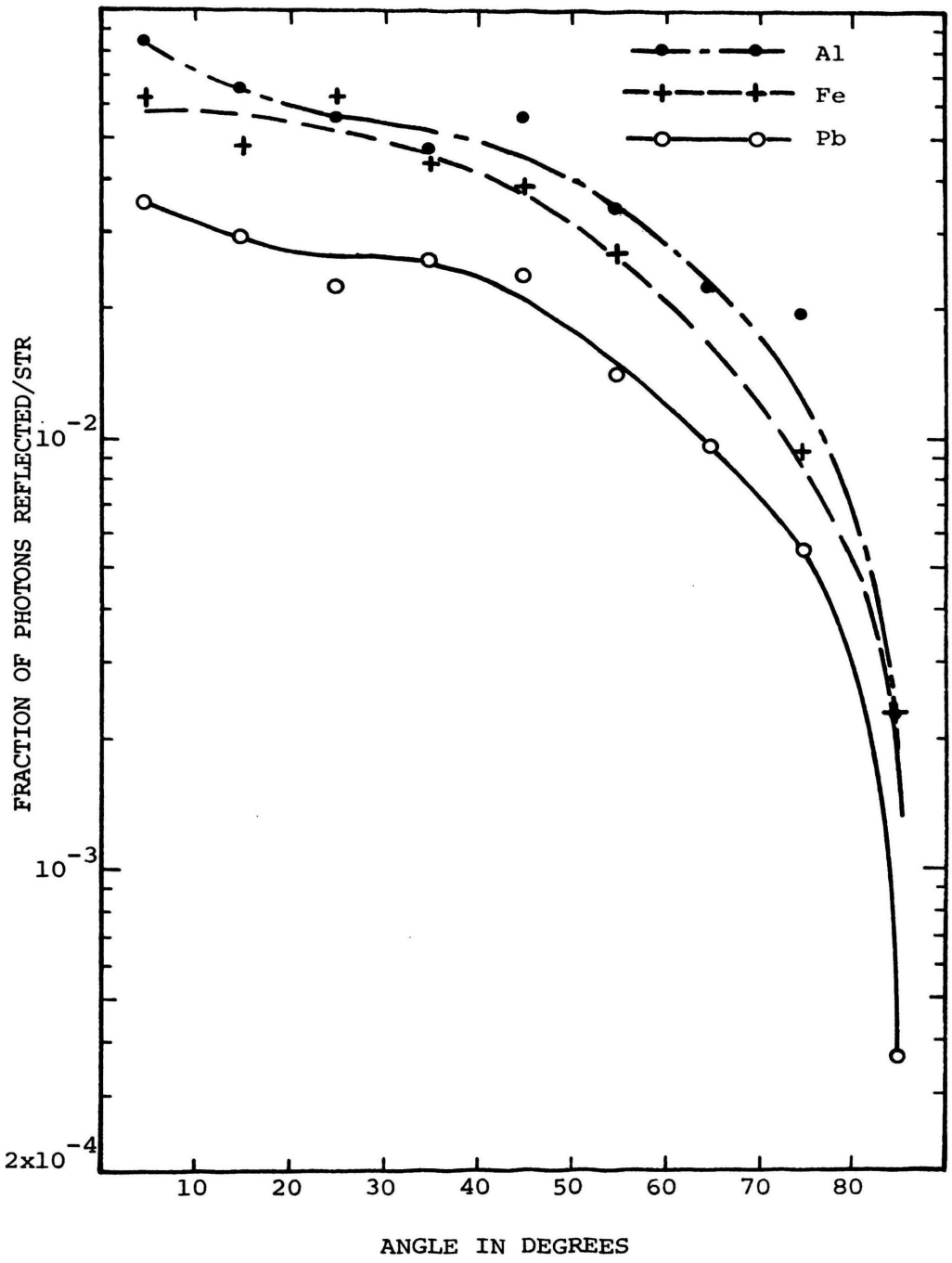

Fig. 5. Differential Number Albedo, $\alpha_N(E_0,\theta)$, for 10 MeV Incident Gammas.

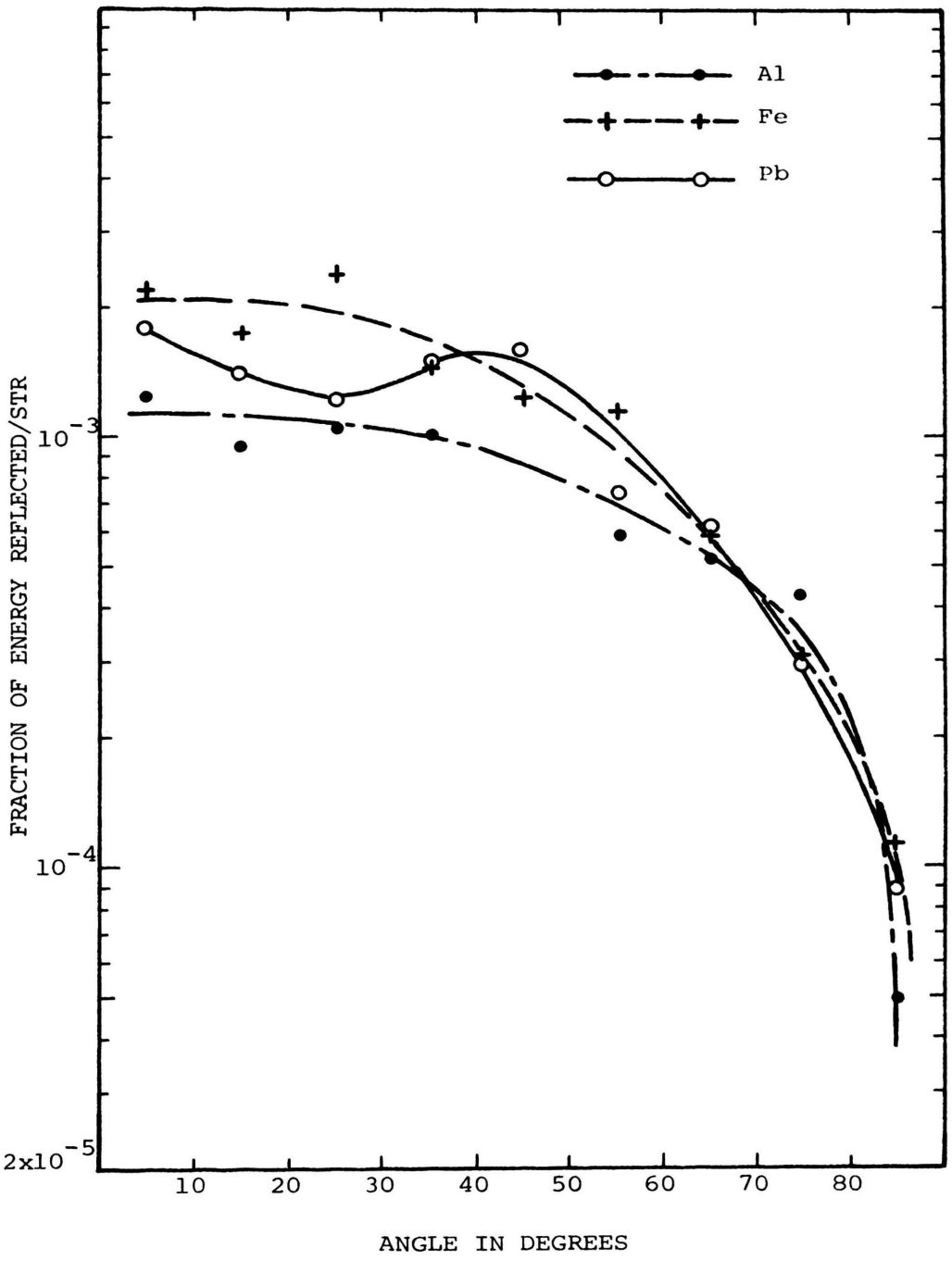

Fig. 6. Differential Energy Albedo, $\alpha_E(E_0,\theta)$, for 10 MeV Incident Gammas.

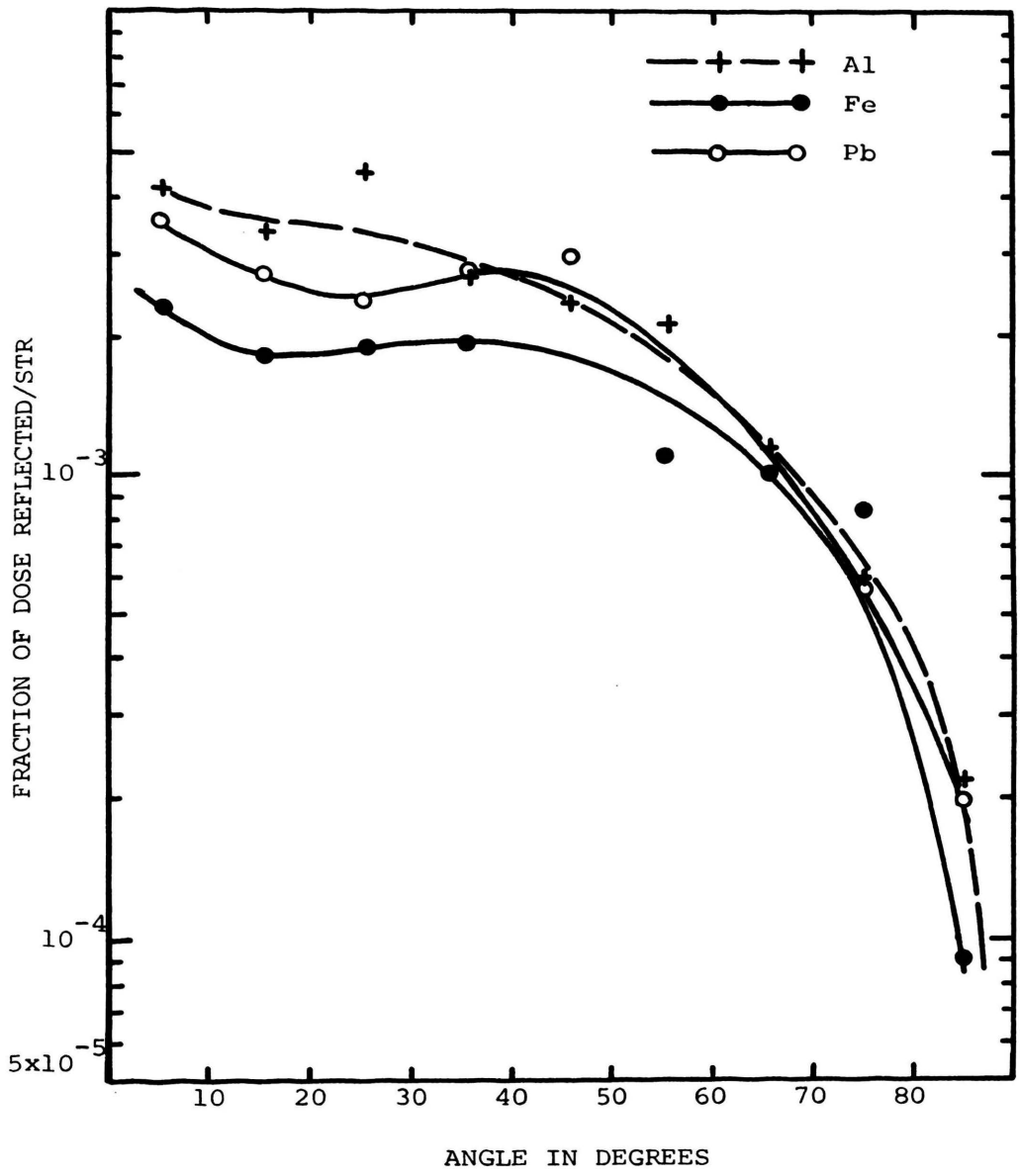

Fig. 7. Differential Dose Albedo, $\alpha_D(E_0,\theta)$, for 10 MeV Incident Gammas.

.41 MeV the albedo definitely decreases as Z increases. At 10 MeV the change with Z is much smaller. This is a consequence of the fact that the albedo, in general, changes little with atomic number Z, for incident gamma energies greater than 4 MeV.

C. Differential Energy-Dependent Albedo

Figures 8 and 9 show representative results for the differential energy-dependent albedo.

Figure 8 gives differential albedo (number, energy and dose) for 10 MeV gammas incident on Pb shield. There are two features to notice in this graph. One is the high peak for energies between 0.5 and 1 MeV. The photons in this group are mainly .511 MeV annihilation gammas. For every incident energy above 1.5 MeV this peak is present. The second feature is the rapid decrease of the spectrum at high energies. This is also true for all incident energies. The photons with energy greater than .511 MeV are due to bremsstrahlung. They are not incident photons being backscattered.

Figure 9 shows double differential albedo for reflection angle between 40° and 50°. This angle interval and the energy of 8 MeV was selected for comparison with the only experimental results[11] reported in the literature for this energy. The agreement is very good. Both experiment and calculation give the same fraction of photons in the .5 to 1 MeV energy group. In this case, 94% of the reflected photons are .511 MeV annihilation photons. The gammas above that energy come from bremsstrahlung. The agreement between

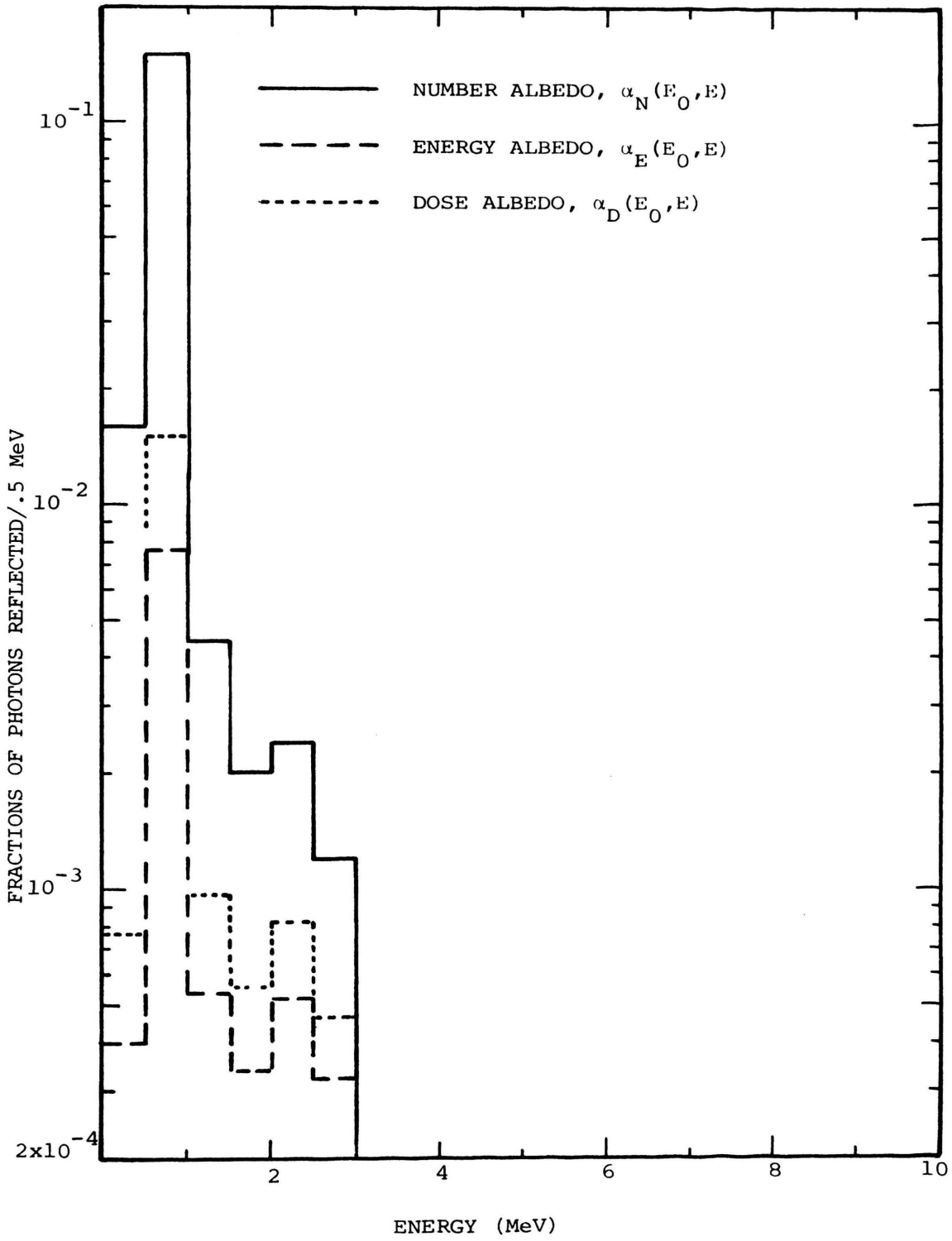

Fig. 8. Differential Energy-Dependent Albedo for 10 MeV Photons Incident on Pb.

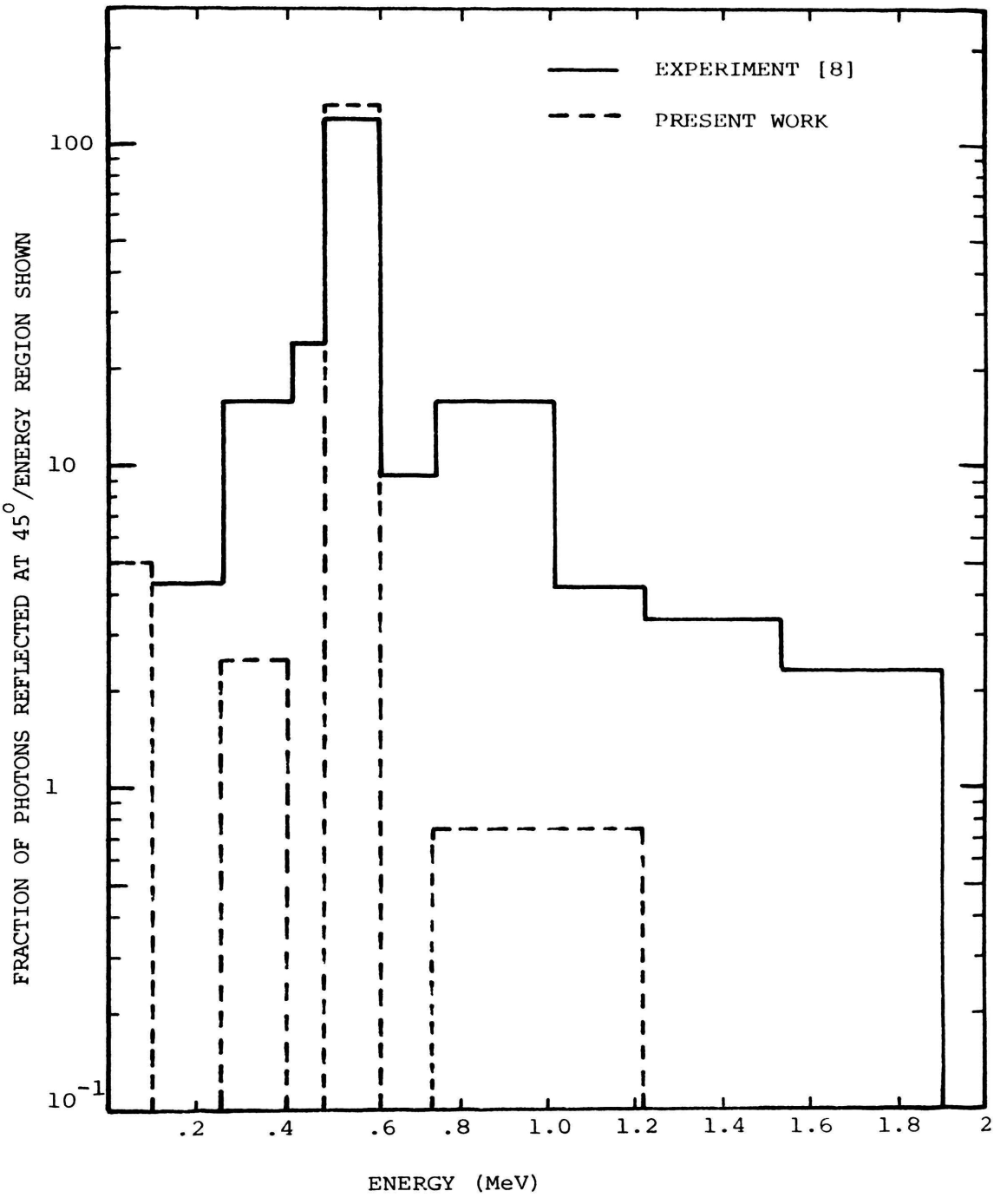

Fig. 9. Double Differential Number Albedo at 45°, $\alpha_N(E_0,E,45^{\circ})$, for 8 MeV Photons Incident on Pb.

the two results is not so good for other energy groups due to large statistical errors.

D. Total Albedo

Figures 10-12 show total albedo for Al, Fe and Pb as a function of incident photon energy. Energy and dose albedo for Al and Fe have a shape somewhat like $\frac{1}{E_0}$. The albedo changes drastically up to 4 MeV but much slower after 4 MeV. The number albedo decreases for Al up to 4 MeV and slightly increases beyond that energy. For Fe, it decreases up to 2 MeV and it increases after that energy.

Figure 12 shows that total albedo for Pb. The increase of the value of albedo after 1 MeV is due to the fast increase of the probability for pair production after 1 MeV. Annihilation gammas have a greater chance of being reflected than incident photons. At higher energies, the albedo changes little because there are no drastic changes in the attenuation coefficients.

Tables I and II indicate the difference in total albedo values when Rayleigh scattering is explicitly considered. This difference could be an increase of up to 12% at high energy. Explicit treatment of Rayleigh scattering means that this effect was not incorporated into the value of Compton scattering but it was treated as an independent event. Since Rayleigh scattering does not change the photon energy, it will tend to keep the particle at a higher energy. It will also tend to increase the

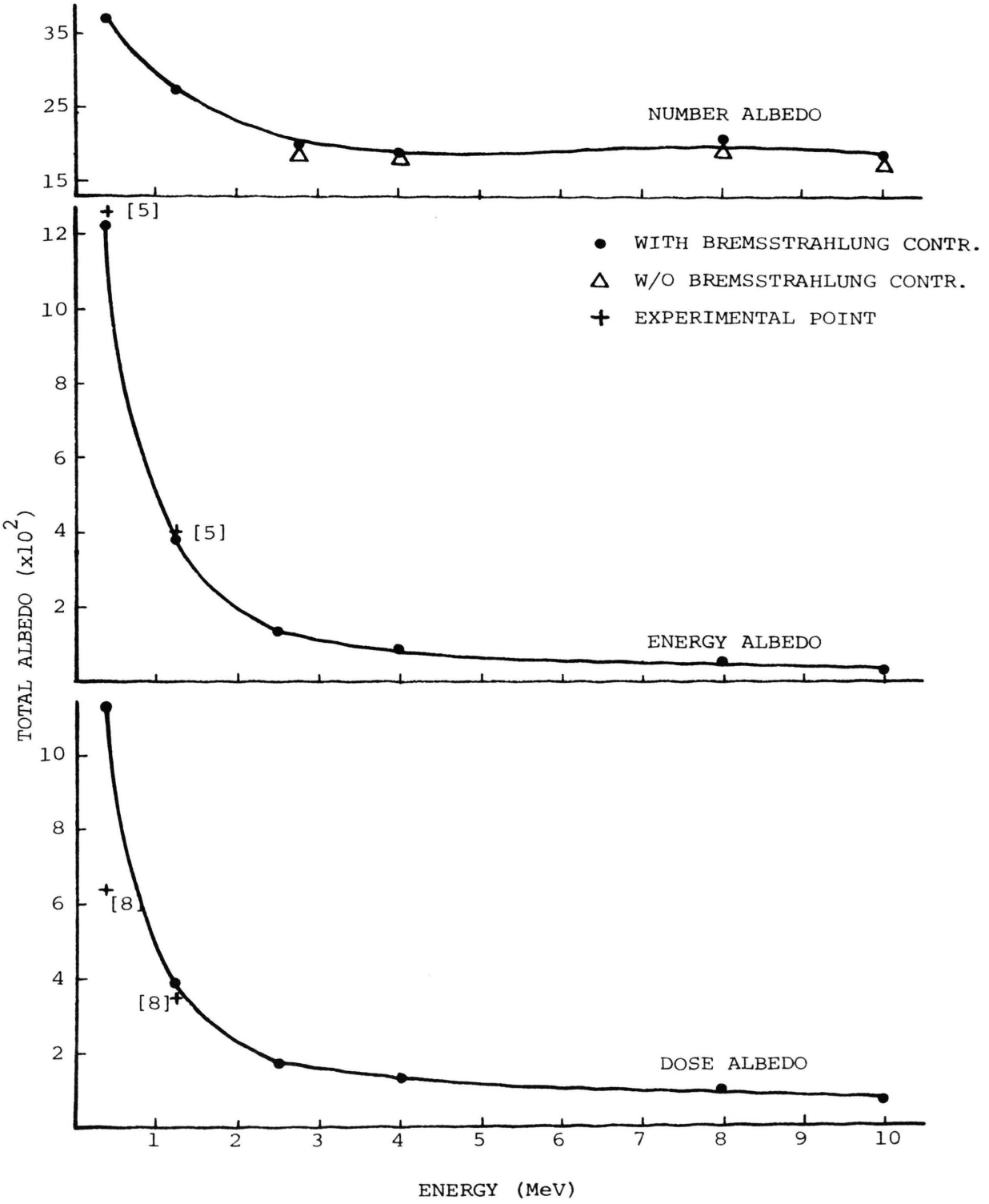

Fig. 10. Total Albedo for Al as Function of Incident Photon Energy.

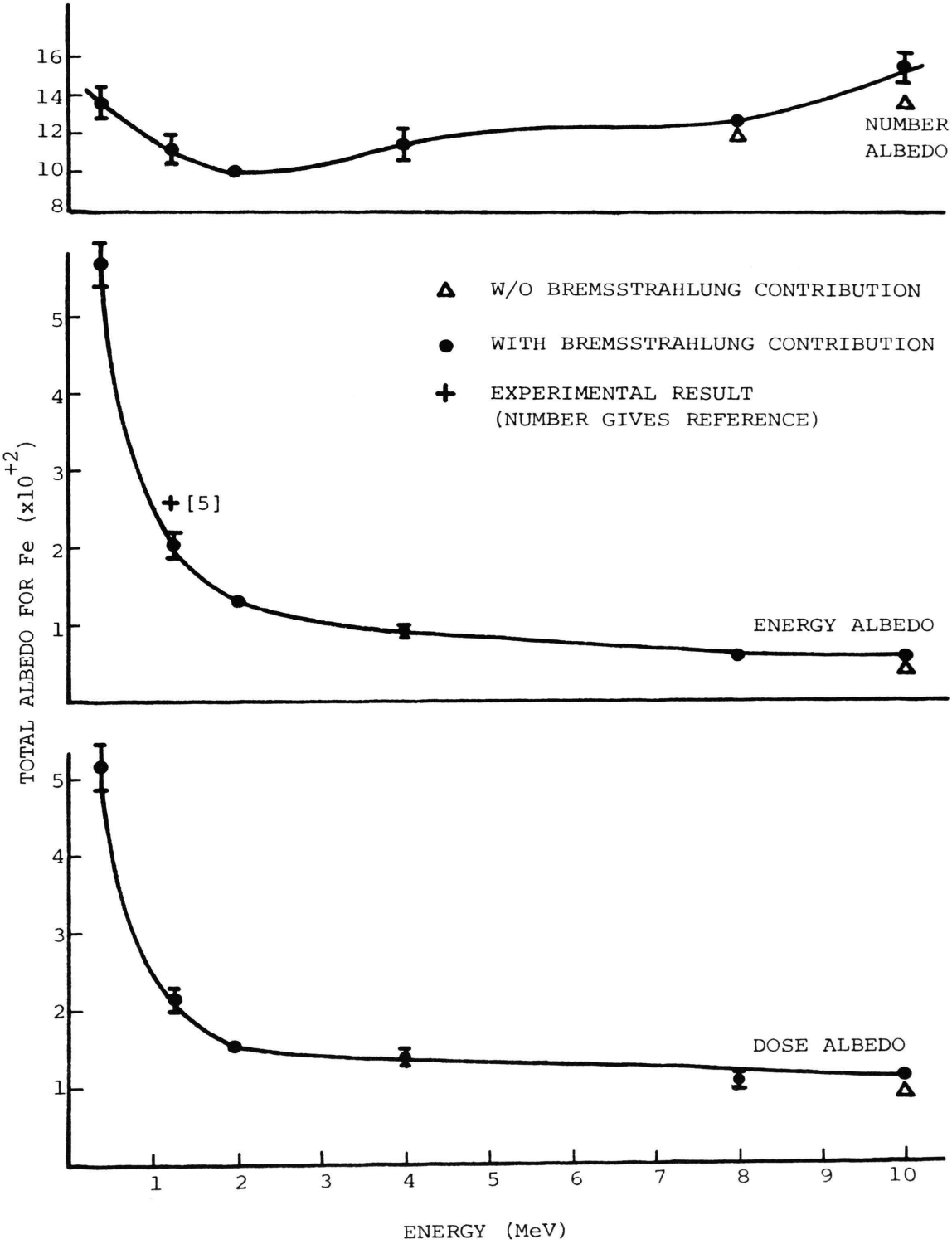

Fig. 11. Total Albedo for Fe as a Function of Incident Photon Energy.

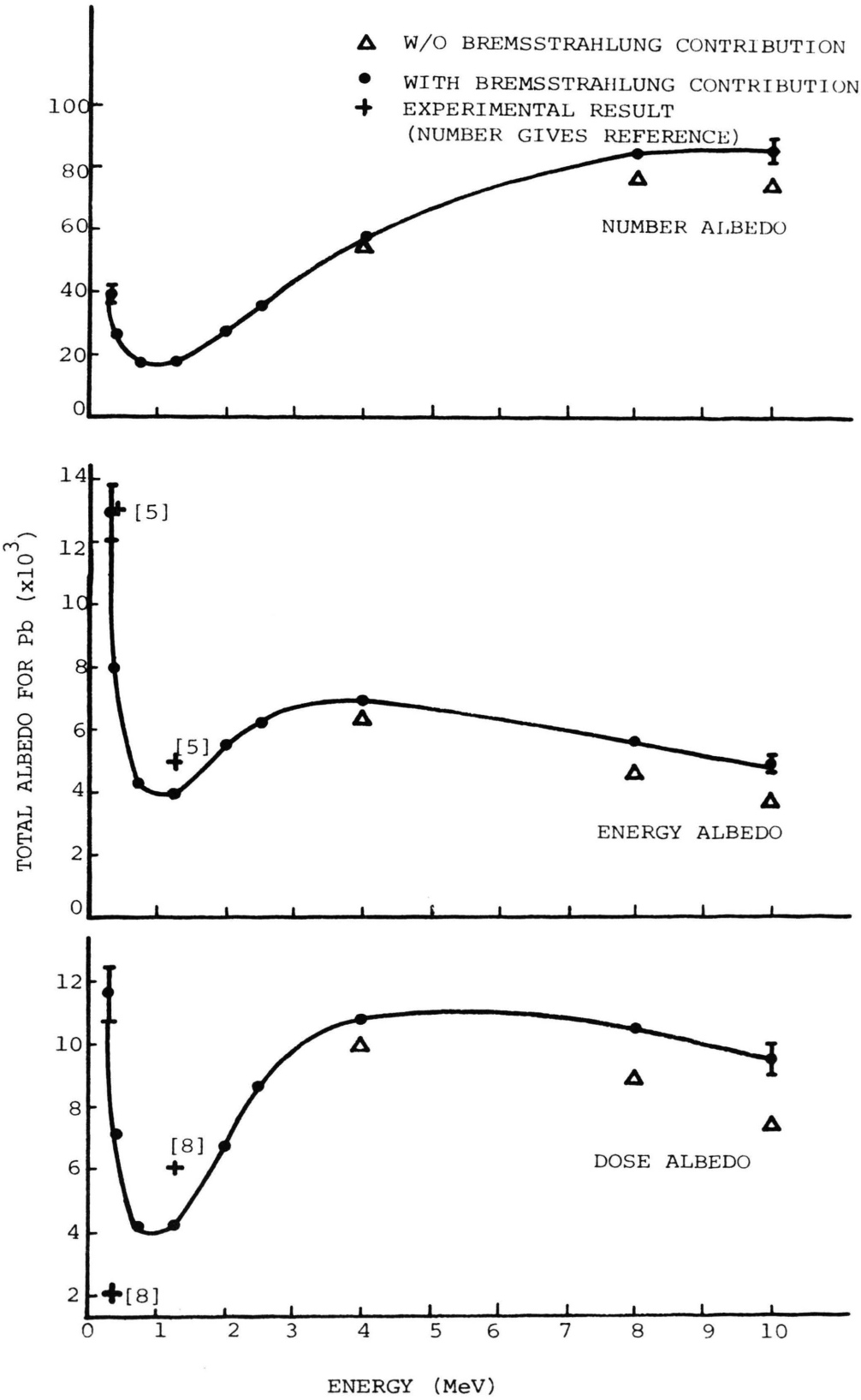

Fig. 12. Total Albedo for Pb as a Function of Incident Photon Energy.

TABLE I. EFFECT OF EXPLICIT RAYLEIGH SCATTERING TREATMENT ON TOTAL ALBEDO FOR Al

Type of Albedo	Photon Energy MeV	Albedo Without Explicit Rayleigh Treatment	Albedo With Explicit Rayleigh Treatment	Change in Percent
	.41	.348 ± 7%	.370 ± 6%	+ 6%
Number	1.25	.257 ± 6%	.276 ± 6%	+ 7%
	8	.216 ± 6%	.210 ± 6%	Negl.
	.41	.118 ± 7%	.123 ± 7%	Negl.
Energy	1.25	.0340 ± 7%	.0382 ± 7%	+ 11%
	8	.0059 ± 8%	.0055 ± 8%	Negl.
	.41	.108 ± 7%	.111 ± 7%	Negl.
Dose	1.25	.0351 ± 7%	.0394 ± 7%	+ 11%
	8	.0093 ± 8%	.01 ± 8%	Negl.

Negl. - Negligible

TABLE II. EFFECT OF EXPLICIT RAYLEIGH SCATTERING TREATMENT ON TOTAL ALBEDO FOR LEAD

Type of Albedo	Photon Energy MeV	Albedo Without Explicit Rayleigh Treatment	Albedo With Explicit Rayleigh Treatment	Change in Percent
	.41	.0266 ± 9%	.0260 ± 9%	Negl.
Number	1.25	.0190 ± 9%	.018 ± 10%	Negl.
	8	.0758 ± 5%	.085 ± 5%	11%
	.41	.0082 ± 9%	.0079 ± 9%	Negl.
Energy	1.25	.0041 ± 10%	.0039 ± 10%	Negl.
	8	.00497 ± 6%	.00557 ± 5%	+ 11%
	.41	.0074 ± 9%	.0071 ± 9%	Negl.
Dose	1.25	.0044 ± 10%	.0042 ± 10%	Negl.
	8	.00928 ± 6%	.0104 ± 5%	+ 11%

Negl. - Negligible

scattering events, thus increasing the chance of reflection. Therefore, explicit treatment of Rayleigh scattering should tend to increase the value of albedo. The results of the calculation verify this conclusion. The inclusion of Rayleigh scattering brings the results of the calculation to closer agreement with experiment.

Tables III, IV and V show the bremsstrahlung contribution to the total albedo. This contribution is more pronounced at high incident photon energy for high Z material. It becomes 15% of the total dose albedo for 8 MeV gammas incident on Pb.

The X-ray contribution to total albedo is none for Al and Fe since their K shell electron binding energy is less than the cut-off energy of 10 KeV, which is the minimum energy considered in the calculation. For Pb shield, it is significant especially at low energies. For example, 38% of dose albedo at .41 MeV incident photon energy is due to X-ray contribution.

Figures 13-15 show total albedo as a function of atomic number, at three different energies. In general, albedo decreases as atomic number increases.

E. Energy Deposition

Table VI gives the fraction of gamma-ray energy deposition in Al, Fe and Pb shield at different energies of incident photons. This fraction is almost constant for Pb at all photon energies, but for Al and Fe it increases, slightly, with photon energy.

TABLE III. CONTRIBUTION OF BREMSSTRAHLUNG TO TOTAL ALBEDO FOR Al

			Present Work	
Type of Albedo	Photon Energy MeV	Experimental Results	Total Albedo	Bremsstrahlung Contribution % of Total
Number	.41	NA	.370 ± 6%	Negl.
	1.25	NA	.276 ± 6%	Negl.
	8	NA	.210 ± 6%	9%
Energy	.41	.127[5]	.123 ± 7%	Negl.
	1.25	.041[5]	.0382 ± 7%	Negl.
	8	NA	.0055 ± 8%	11%
Dose	.41	.064[8]	.111 ± 7%	Negl.
	1.25	.0375[8]	.0394 ± 7%	Negl.
	8	NA	.01 ± 8%	10%

Negl. - Negligible

NA - Not Available

TABLE IV. CONTRIBUTION OF BREMSSTRAHLUNG TO TOTAL ALBEDO FOR Fe

			Present Work	
Type of Albedo	Photon Energy MeV	Experimental Results	Total Albedo	Bremsstrahlung Contribution % of Total
	.41	NA	.137 ± 6%	Negl.
Number	1.25	NA	.113 ± 7%	Negl.
	8	NA	.132 ± 6%	6%
	.41	.087[5]	.057 ± 6%	Negl.
Energy	1.25	.026[5]	.021 ± 7%	Negl.
	8	NA	.0057 ± 7%	6%
	.41	.042[8]	.052 ± 6%	Negl.
Dose	1.25	.033[8]	.022 ± 7%	Negl.
	8	.0066[11]	.0106 ± 7%	6%

Negl. - Negligible

NA - Not Available

TABLE V. CONTRIBUTION OF BREMSSTRAHLUNG AND X RAYS TO TOTAL ALBEDO FOR Pb

Type of Albedo	Photon Energy MeV	Experimental Results	Present Work Total Albedo	Present Work Bremsstrahlung Contribution % of Total	Present Work X-ray Contribution % of Total
	.41	NA	.026 ± 9%	Negl.	57%
Number	1.25	NA	.018 ± 10%	Negl.	14%
	8	NA	.085 ± 5%	10%	Negl.
	.41	.013 [5]	.0079 ± 9%	Negl.	39%
Energy	1.25	.005 [5]	.0039 ± 10%	2%	4%
	8	NA	.0056 ± 6%	16%	Negl.
	.41	.002 [8]	.0071 ± 9%	Negl.	38%
Dose	1.25	.006 [8]	.0042 ± 10%	2%	4%
	8	.024 [11]	.0104 ± 5%	15%	Negl.

Negl. - Negligible

NA - Not Available

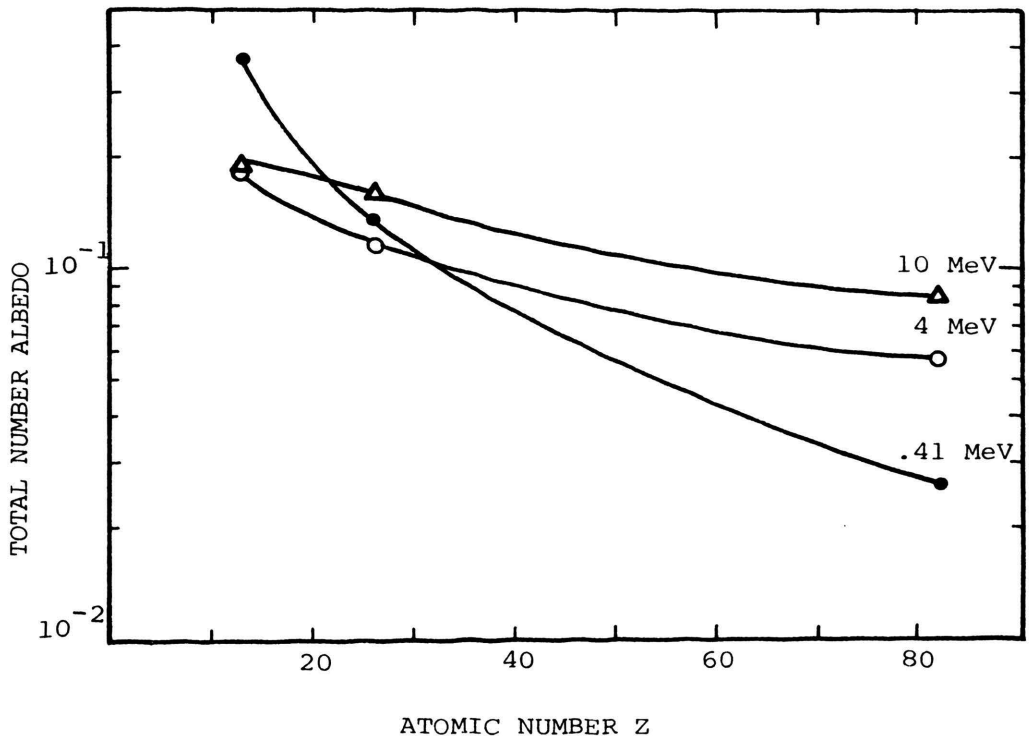

Fig. 13. Total Number Albedo as a Function of Atomic Number.

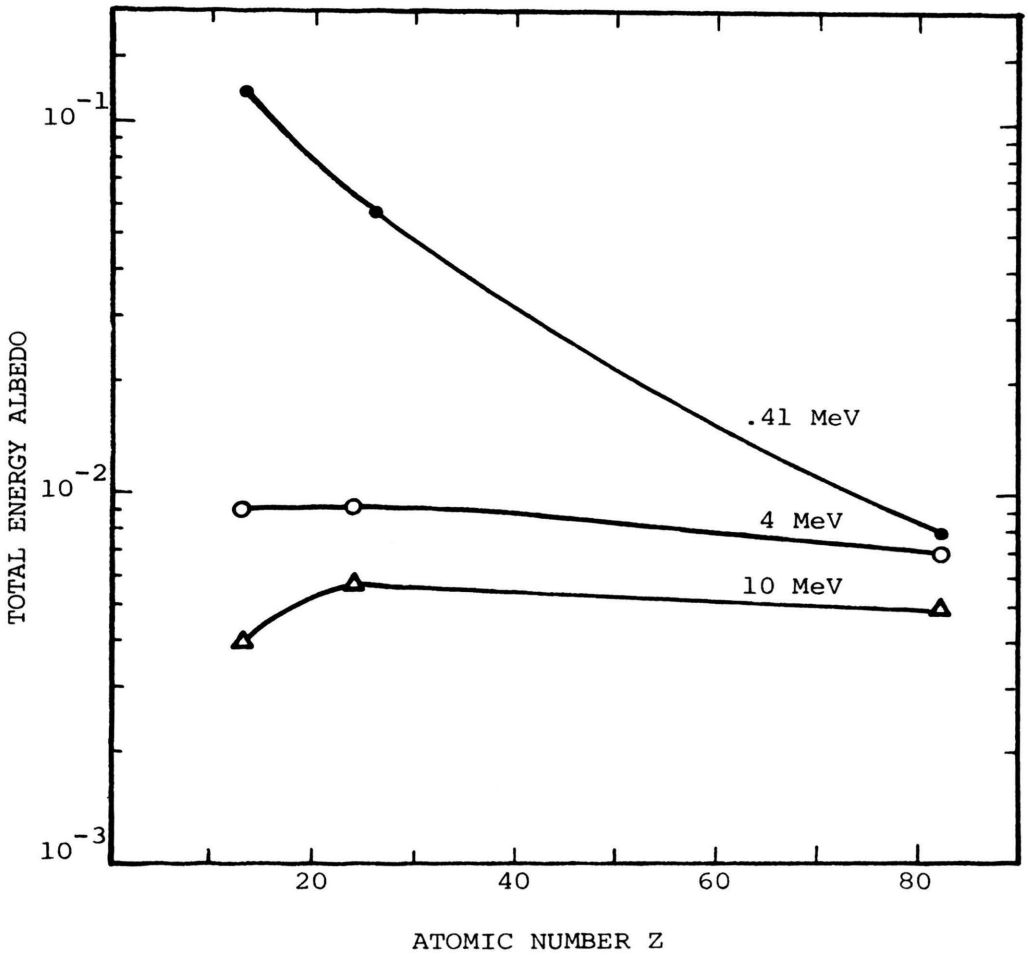

Fig. 14. Total Energy Albedo as a Function of Atomic Number.

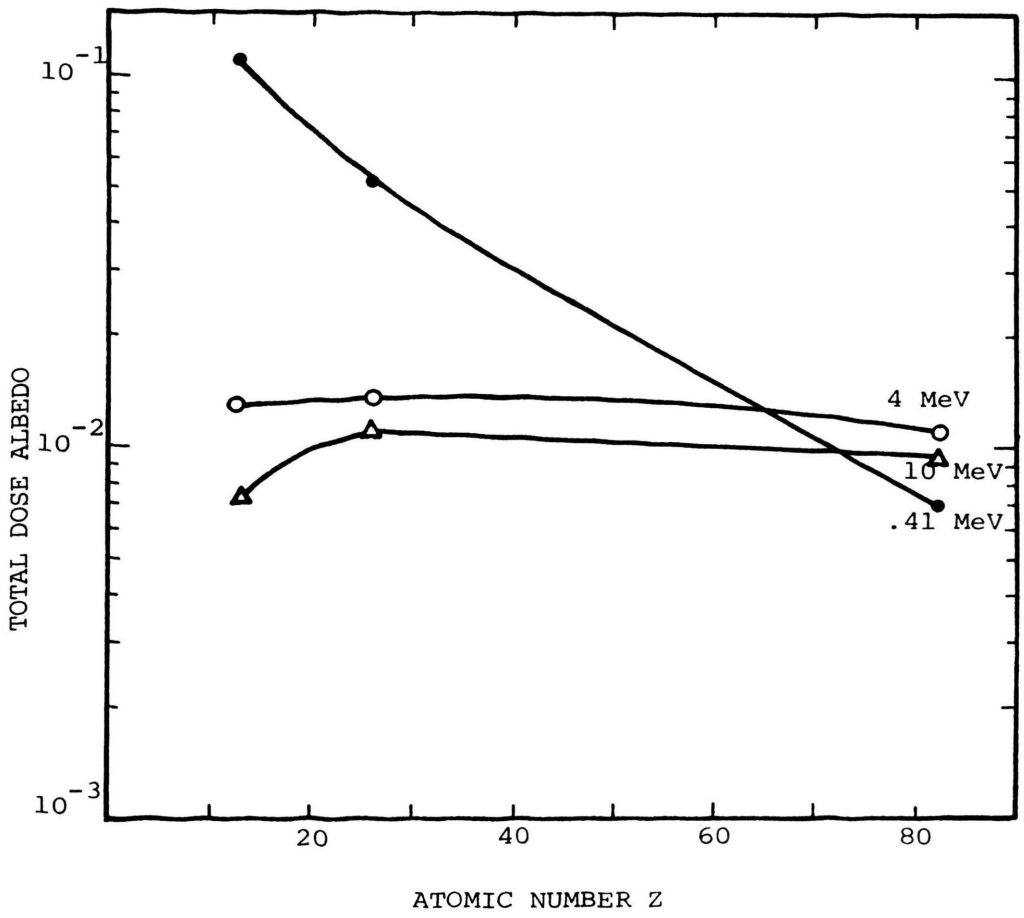

Fig. 15. Total Dose Albedo as a Function of Atomic Number.

TABLE VI. FRACTION OF GAMMA-RAY ENERGY DEPOSITED IN THE SHIELD

Photon Energy MeV	Al 4 M.F.P.	Fe 3 M.F.P.	Pb 2 M.F.P.
.41	78%	80%	80%
1.25	91%	85%	79%
2	-	87%	78%
2.5	94%	-	79%
4	94%	89%	80%
8	96%	-	79%
10	93%	91%	80%

Figure 16 shows a representative example of energy deposition inside the shield. Although the total fraction of energy deposited is about 80% for all three materials, the areas under the histogram in Figure 16 look quite different in size, because the thickness of the regions is quite different for the three materials.

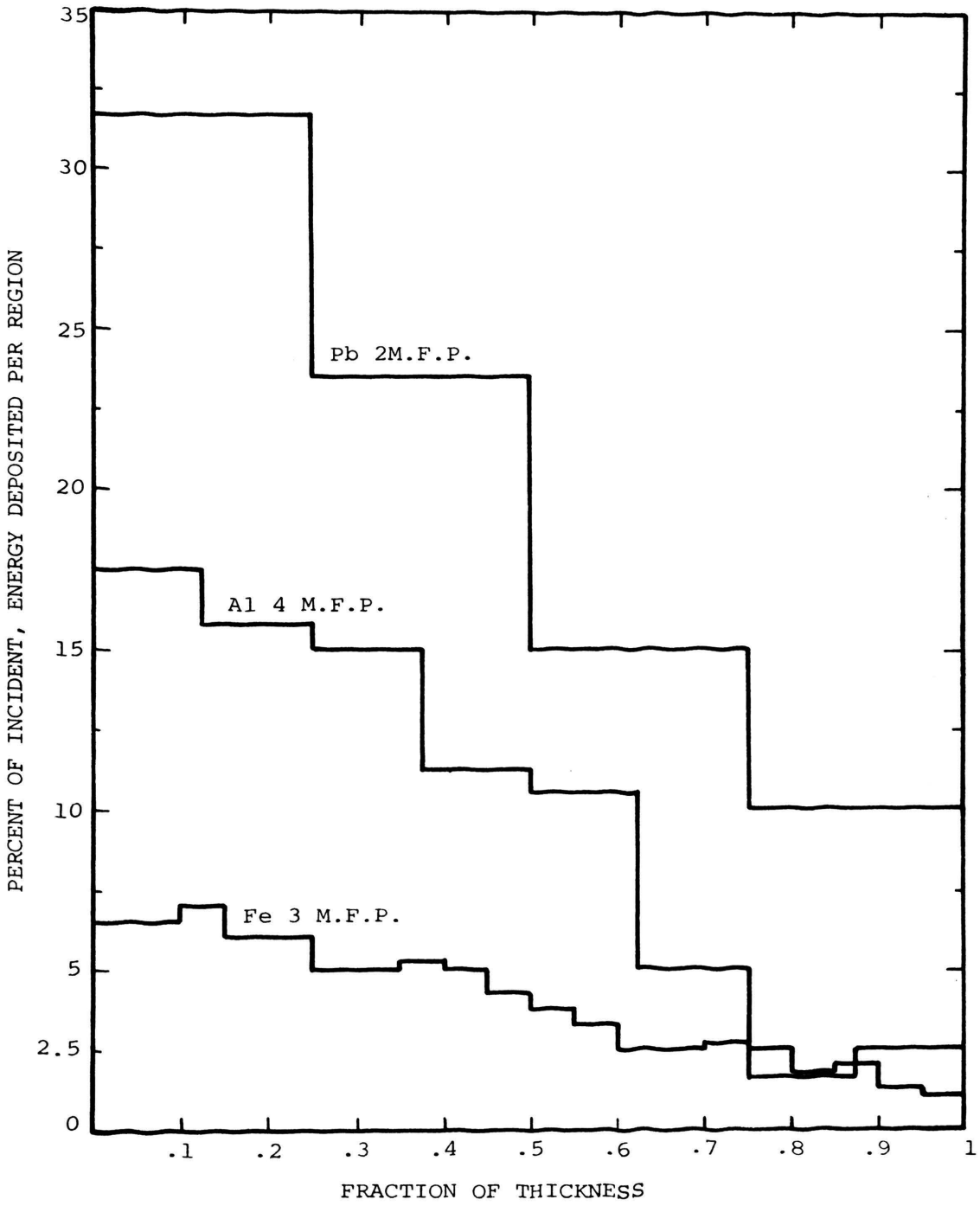

Fig. 16. Percent of Incident Energy Deposited per Incidental Region. Incident Energy E = .41 MeV.

IV. CONCLUSIONS AND RECOMMENDATIONS

In studying gamma ray albedo the secondary radiations should be considered since their contribution to the results is significant in many cases. Annihilation gammas and bremsstrahlung contribution to albedo are more pronounced for high Z material at high energies while X rays contribute more at low energies. Rayleigh scattering ought to be treated explicitly since the results agree better with experiment if this is done. Fraction of γ-energy deposited in the shield is constant for Pb, at various photon energies, but it shows an increase with energy for Al shield.

The computer program, which was developed, can calculate double differential albedo and for multiple layer shields. It is recommended that these studies be carried out, if the expense of computer time necessary can be covered.

BIBLIOGRAPHY

1. Selph, W. E., "Neutron and Gamma Ray Albedos", ORNL-RSIC-21(DASA-189-2) Oak Ridge National Laboratory, 1968.

2. Vogt, Hans-Gerrit, "Method for the Determination of Differential Albedos for 1-17 MeV Photons", Ph.D. thesis, Hannover Engineering University, Germany, 1971.

3. "Radiation Shielding for Nuclear Engineers", N. M. Schaeffer, Editor, TID-25951, U.S.A.E.C. (1973).

4. Hayward, E. and Hubbell, J. H., "The Backscattering of the Co-60 Gamma Rays From Infinite Media", J. Appl. Phys., 25, 4, 506 (1954).

5. Bulatov, B. P. and Garusov, E. A., "Co-60 and Au-198 Gamma Ray Albedo for Various Materials", J. Nucl. Energy, Part A: Reactor Science, 11, 159 (1960).

6. Clifford, C. E., "Angular Differential Dose Albedo Measurements for .66 MeV Gamma Incident on Concrete, Iron and Lead", Can. J. Phys., 42, 957 (1964).

7. Haggmark, L. G., Jones, T. H., Scofield, N. E. and Gurney, W. J., "Differential Dose-Rate Measurement of Backscattered Gamma Rays From Concrete, Aluminum and Steel", Nucl. Sci. Eng., 23, 138 (1965).

8. Steyn, J. J. and Andrews, D. G., "Experimental Differential Number, Energy and Exposure Albedos for Semi-Infinite Media for Normally Incident Gamma Photons", Nucl. Sci. Eng., 27, 318 (1967).

9. Mizukami, K., Matsumoto, T. and Hyodo, T., "Backscattering of Gamma Rays From Polyethylene, Aluminum and Lead Slabs", J. Nucl. Sci. Tech., 4, 12, 607 (1967).

10. Hassler, L. A. and Johnson, W. R., "Backscattered Spectra in High-Energy Gamma-Ray Albedo Measurements", Trans. Am. Nucl. Soc., 396, 14, 1 (1971)

11. Johnson, W. R., Thompson, W. L., Risher, D. H., Hassler, L. A., and Royers, J. E., "Gamma Ray Transport at 6 and 8 MeV", 4th International Conference on Radiation Shielding (Paris, October 9-13, 1972).

12. Thompson, W. L., "Gamma-Ray and Electron Transport by Monte Carlo", Trans. Am. Nucl. Soc., 978, 15, 2 (1972).

BIBLIOGRAPHY (cont.)

13. Preiss, K. and Livnat, R., "The Distribution of Backscattered Gamma-Ray Photons in the Scattering Medium", Nucl. Eng. Des. 24, 258 (1973).

14. Hayward, E. B. and Hubbell, J., "The Albedo of Various Materials for 1 MeV Photons", Phys. Rev. 93, 955 (1954).

15. Perkins, J. F., "Monte-Carlo Calculations of Gamma-Ray Albedos of Concrete and Aluminum", J. Appl. Phys. 26, 655 (1955).

16. Berger, M. J., Doygett, J., "Reflection and Transmission of Gamma Radiation by Barriers: Semianalytic Monte Carlo Calculation", J. Res. Nat. Bur. Std. 56, 2, 89 (1956).

17. Berger, M. J. and Raso, D. J., "Monte-Carlo Calculations of Gamma-Ray Backscattering", Rad. Res., 12, 20 (1960).

18. Leimdorfer, M., "The Backscattering of Gamma Radiation From Plane Concrete Walls", Nucl. Sci. Eng. 17, 345 (1963).

19. Leimdorfer, M., "The Backscattering of Gamma Radiation From Spherical Concrete Walls", Nucl. Sci. Eng. 17, 352 (1963).

20. Raso, D. J., "Monte-Carlo Calculations on the Reflection and Transmission of Scattered Gamma Rays", Nucl. Sci. Eng. 17, 411 (1963).

21. Pozdneev, D. B., "Scattering of Gamma Radiation by Fe Barriers", Sov. At. En. 22, 385 (1967).

22. Viktorov, A. A., Efimenko, B. A., Zolotukhin, V. G., Klimanov, V. A. and Mashkovich, V. P., "Differential Albedo for Gamma Rays From a Point Undirectional Source", Sov. At. En. 23 #3, 197 (1967).

23. Razani, A., "A Monte Carlo Method for Radiation Transport Calculations", J. Nucl. Sci. Tech., 9 (9), 551 (1972).

24. Chilton, A. B. and Huddleston, C. M., "A Semiempirical Formula for Differential Dose Albedo for Gamma Rays on Concrete", Nucl. Sci. Eng. 17, 419 (1963).

25. Smith, C. V. and Scofield, N. E., "Gamma-Ray Albedo Calculations Using Moments Method", Nucl. Sci. Eng. 47, 1 (1972).

26. Hubbell, J. H., "Photon Cross Sections, Attenuation Coefficients and Energy Absorption Coefficients From 10 KeV to 100 GeV", NSRDS-NBS 29 (1969).

BIBLIOGRAPHY (cont.)

27. Evans, R. D., "The Atomic Nucleus", McGraw-Hill Company, New York (1955).

28. Kahn, H., "Applications of Monte Carlo", Rand Corporation Research Memorandum, RM 1237-AEC, 19 April 1954, Revised 27 April 1956.

29. Tabata, R. I. and Okabe, S., "Generalized Semiempirical Equations for the Extrapolated Range of Electrons", Nucl. Inst. Meth., 103, 85 (1972).

30. Berger, M. J. and Seltzer, S. M., "Tables of Energy Losses and Ranges of Electrons and Positrons", NASA SP-3012 (1964).

31. Roy, R. R. and Reed, R. D., "Interactions of Photons and Leptons with Matter", Academic Press, New York (1968).

32. Dance, W. E., Rester, D. E., Farmer, B. J., Johnson, J. H. and Baggerly, L. L., "Bremsstrahlung Produced in Thick Aluminum and Iron Targets by .t to 2.8 MeV Electrons", J. Appl. Phys., 39, 288 (1968).

33. Rester, D. H., Dance, W. E. and Derrickson, J. H., "Thick Target Bremsstrahlung by Electron Bombardment of Targets of Be, Sn and Au in the Energy Range .2-2.8 MeV", J. Appl. Phys., 41, 2682 (1970).

VITA

Ezatholah Aslani-Amoli was born in Amol, Iran on December 31, 1945. He received his primary education in Amol and secondary education in Tehran, Iran. He received his B.S. in Physics from Tehran University in June 1966. Then, he served in the Iranian Army as 2nd Lieutenant until September 1968. He worked as research assistant at the Tehran University Nuclear Center until December 1969 at which time he received his M.S. degree in Physics. In 1970 he came to the United States. He has been enrolled in the Graduate School of the University of Missouri-Rolla since September 1970.